SHAPE OPTIMIZATION FOR 3D ELECTRICAL IMPEDANCE TOMOGRAPHY

Karsten Eppler
Weierstraß Institut für Angewandte Analysis und Stochastik
Mohrenstr. 39, 10117 Berlin, Germany.
eppler@math.wias-berlin.de

Helmut Harbrecht*
Institut für Informatik und Praktische Mathematik, Christian–Albrechts–Universität zu Kiel,
Olshausenstr. 40, 24098 Kiel, Germany.
hh@numerik.uni-kiel.de

Abstract In the present paper we consider the identification of an obstacle or void of different conductivity included in a three-dimensional domain by measurements of voltage and currents at the boundary. We reformulate the given identification problem as a shape optimization problem. Since the Hessian is compact at the given hole we apply a regularized Newton scheme as developed in [14]. All information of the state equation required for the optimization algorithm can be derived by boundary integral equations which we solve numerically by a fast wavelet Galerkin scheme. Numerical results confirm that the proposed regularized Newton scheme yields a powerful algorithm to solve the considered class of problems.

Keywords: Electrical impedance tomography, Newton method, regularization, boundary integral equations, wavelets.

*This research has been carried out when the second author stayed at the Department of Mathematics, University of Utrecht, Netherlands, supported by the EU-IHP project *Nonlinear Approximation and Adaptivity: Breaking Complexity in Numerical Modelling and Data Representation*

Introduction

Let $D \subset \mathbb{R}^3$ denote a bounded domain with boundary $\partial D = \Sigma$ and assume the existence of a simply connected subdomain $S \subset D$, consisting of material with constant conductivity, essentially different from the likewise constant conductivity of the material in the subregion $\Omega = D \setminus \overline{S}$. We consider the identification problem of this inclusion if the Cauchy data of the electrical potential u are measured at the boundary Σ , i.e., if a single pair $f = u|_\Sigma$ and $g = (\partial u/\partial \mathbf{n})|_\Sigma$ is known.

The problem under consideration is a special case of the general conductivity reconstruction problem and is severely ill-posed. It has been intensively investigated as an inverse problem. We refer for example to Hettlich and Rundell [22]and Chapko and Kress [4]for numerical algorithms and to Friedmann and Isakov [15]as well as Alessandrini, Isakov and Powell [1]for particular results concerning uniqueness. Moreover, we refer to Brühl and Hanke [2–3]for methods using the complete Dirichlet–to–Neumann operator at the outer boundary. We emphasize that we focus in the present paper on exact measurements and do not consider noisy data.

In [24], Roche and Sokolowski have been introduced a formulation as shape optimization problem. However, we have proven in [14]that the shape Hessian degenerates at the optimal domain. Nevertheless, using second order information in terms of a regularized Newton scheme yieled promising results in comparison to gradient based methods. In particular, the method converges faster and provides higher accuracy. The present paper intends to extent these results to three dimensions.

We employ boundary integral representations of the shape functional, its gradient and its Hessian. After transforming the state equation to a boundary integral equation, we are able to perform all computations just on the boundary of the domain under consideration. To obtain a finite dimensional optimization problem we assume the inclusion starshaped and discretize its boundary by spherical harmonics. The boundary integral equations are solved efficiently by a fast wavelet Galerkin scheme which computes the approximate solutions within linear complexity [6, 21, 25].

The present paper is organized as follows. In Section 1.1 we present the physical model and reformulate the identification problem as shape optimization problem. We compute the gradient and the Hessian of the given shape functional and show how to use boundary integral equations to compute them. In Section 1.2 we discretize the boundary of the inclusion and replace the infinite dimensional optimization problem by finite dimensional one. Moreover, we propose a wavelet based fast boundary

element method to compute the shape functional as well as its gradient and Hessian. In Section 1.3, we present a numerical experiment in which we compare the regularized Newton method with a quasi Newton method.

1. Shape problem formulation

1.1 The physical model

Let $D \in \mathbb{R}^3$ be a simply connected domain with boundary $\Sigma = \partial D$ and assume that an unknown simply connected inclusion S with regular boundary $\Gamma = \partial S$ is located inside the domain D satisfying $\operatorname{dist}(\Sigma, \Gamma) > 0$, cf. Figure 1. To determine the inclusion S we measure for a given current distribution $g \in H^{-1/2}(\Sigma)/\mathbb{R}$ the voltage distribution $f \in H^{1/2}(\Sigma)$ at the boundary Σ. Hence, we are seeking a domain $\Omega := D \setminus \overline{S}$ and an associated harmonic function u, satisfying the system of equations

$$\begin{aligned} \Delta u &= 0 && \text{in } \Omega, \\ u &= 0 && \text{on } \Gamma, \\ u &= f && \text{on } \Sigma, \\ \frac{\partial u}{\partial \mathbf{n}} &= g && \text{on } \Sigma. \end{aligned}$$

This system denotes an overdetermined boundary value problem which admits a solution only for the true inclusion S.

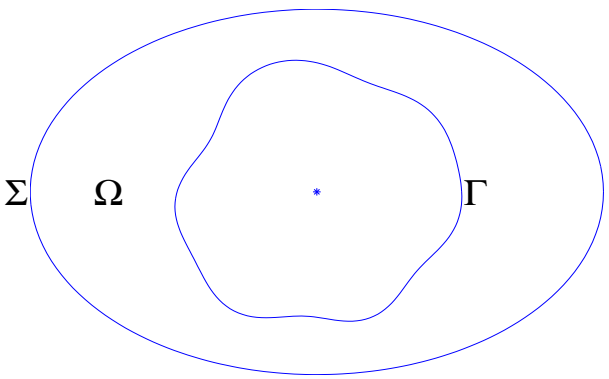

Figure 1. The domain Ω and its boundaries Γ and Σ.

Following Sokolowski and Roche [24], we introduce the auxiliary harmonical functions v and w satisfying

$$\begin{aligned} \Delta v = 0 \qquad & \Delta w = 0 \qquad && \text{in } \Omega, \\ v = 0 \qquad & w = 0 \qquad && \text{on } \Gamma, \\ \frac{\partial v}{\partial \mathbf{n}} = g \qquad & w = f \qquad && \text{on } \Sigma, \end{aligned} \tag{1}$$

and consider the following shape optimization problem

$$J(\Omega) = \int_\Omega \|\nabla(v-w)\|^2 d\mathbf{x} = \int_\Sigma \left(g - \frac{\partial w}{\partial \mathbf{n}} \right) (v-f) d\sigma \to \inf . \tag{2}$$

Herein, the infimum has to be taken over all domains including a void with sufficiently regular boundary. We refer to Roche and Sokolowski [24]for the existence of optimal solutions with respect to this shape optimization problem.

1.2 Shape calculus

For sake of clearness in representation, we repeat the shape calculus concerning the problem under consideration by means of boundary variations. The shape calculus is in complete analogy to the two-dimensional one in [14]. For a survey on the shape calculus based on the material derivative concept, we refer the reader to Sokolowski and Zolesio [26]and Delfour and Zolesio [9]and the references therein.

Let the underlying variation fields $\mathbf{V}$ be sufficiently smooth such that $C^{2,\alpha}$-regularity is preserved for all perturbed domains. Moreover, for sake of simplicity, we assume in addition that the outer boundary and the measurements are sufficiently regular such that the state functions $v = v(\Omega)$ and $w = w(\Omega)$ satisfy

$$v, w \in C^{2,\alpha}(\Omega). \tag{3}$$

Then, a formal differentiation of (2) in terms of local derivatives yields immediately

$$dJ(\Omega)[\mathbf{V}] = \int_\Gamma \langle \mathbf{V}, \mathbf{n} \rangle \|\nabla(v-w)\|^2 d\sigma + 2 \int_\Omega \langle \nabla(v-w), \nabla(dv-dw) \rangle d\mathbf{x},$$

where the local shape derivatives $dv = dv[\mathbf{V}]$ and $dw = dw[\mathbf{V}]$ satisfy

$$\begin{aligned} \Delta dv = 0 \qquad & \Delta dw = 0 \qquad && \text{in } \Omega, \\ dv = -\langle \mathbf{V}, \mathbf{n} \rangle \frac{\partial v}{\partial \mathbf{n}} \qquad & dw = -\langle \mathbf{V}, \mathbf{n} \rangle \frac{\partial w}{\partial \mathbf{n}} \qquad && \text{on } \Gamma, \\ \frac{\partial dv}{\partial \mathbf{n}} = 0 \qquad & dw = 0 \qquad && \text{on } \Sigma. \end{aligned} \tag{4}$$

The boundary integral representation of the shape gradient is now obtained via repeated integration by parts

$$\begin{aligned} dJ(\Omega)[\mathbf{V}] &= \int_\Gamma \langle \mathbf{V}, \mathbf{n} \rangle \{ \|\nabla v\|^2 - \|\nabla w\|^2 \} d\sigma \\ &= \int_\Gamma \langle \mathbf{V}, \mathbf{n} \rangle \left[\left(\frac{\partial v}{\partial \mathbf{n}} \right)^2 - \left(\frac{\partial w}{\partial \mathbf{n}} \right)^2 \right] d\sigma, \end{aligned} \tag{5}$$

cf. [14, 24]. The identity $\nabla v\big|_\Gamma = \partial v / \partial \mathbf{n}$, and likewise for w, issues from the homogeneous Dirichlet boundary condition of the state equation (1). Moreover, note that, as an immediate consequence of the shape calculus, (5) implies an simplified first order necessary condition

$$\frac{\partial v}{\partial \mathbf{n}} = \frac{\partial w}{\partial \mathbf{n}} \qquad \text{on } \Gamma. \tag{6}$$

In the case of a hole S which is starshaped with respect to a certain pole $\mathbf{p}$, the boundary $\Gamma = \partial S$ can be parametrized by a radial function r living on the sphere with radius one around the pole. Without loss of generality we assume throughout this paper this pole to be $\mathbf{0}$. Then, each point $\mathbf{x} \in \Gamma$ is represented uniquely by $\mathbf{x} = r(\widehat{\mathbf{x}}) \cdot \widehat{\mathbf{x}}$, where

$$\widehat{\mathbf{x}} := \frac{\mathbf{x}}{\|\mathbf{x}\|} \in \mathbb{S} := \{ \mathbf{x} \in \mathbb{R}^3 : \|\mathbf{x}\| = 1 \}.$$

As one readily verifies, the outer normal of Ω at the point $\mathbf{x} \in \Gamma$ is given by

$$\mathbf{n}(\mathbf{x}) = \frac{\nabla_{\mathbb{S}} r(\widehat{\mathbf{x}}) - r(\widehat{\mathbf{x}}) \cdot \widehat{\mathbf{x}}}{\sqrt{r^2(\widehat{\mathbf{x}}) + \|\nabla_{\mathbb{S}} r(\widehat{\mathbf{x}})\|^2}} \tag{7}$$

where the surface gradient $\nabla_{\mathbb{S}}$ with respect to the sphere is defined as

$$\nabla_{\mathbb{S}} r(\widehat{\mathbf{x}}) = \nabla r(\widehat{\mathbf{x}}) - \langle \widehat{\mathbf{x}}, \nabla r(\widehat{\mathbf{x}}) \rangle \cdot \widehat{\mathbf{x}}.$$

Note that there holds in particular $\langle \nabla_{\mathbb{S}} r(\widehat{\mathbf{x}}), \widehat{\mathbf{x}} \rangle = 0$.

We choose the perturbation field $\mathbf{V}$ such that $\mathbf{V}(\mathbf{x}) = dr(\widehat{\mathbf{x}}) \cdot \widehat{\mathbf{x}}$. Thus, the shape gradient (5) can be expressed equivalently in local coordinates as

$$dJ(\Omega)[dr] = \int_{\mathbb{S}} dr(\widehat{\mathbf{x}})\, r^2(\widehat{\mathbf{x}}) \left[\left(\frac{\partial w}{\partial \mathbf{n}} \right)^2 - \left(\frac{\partial v}{\partial \mathbf{n}} \right)^2 \right] d\sigma, \tag{8}$$

where the minus sign issues from the fact that $\langle \widehat{\mathbf{x}}, \mathbf{n} \rangle = -r / \sqrt{r^2 + \|\nabla_{\mathbb{S}} r\|^2}$ according to (7).

LEMMA 1 *The shape Hessian is given by*

$$
\begin{aligned}
d^2J(\Omega)[dr_1, dr_2] = \int_{\mathbb{S}} 2r\, dr_1\, dr_2 & \left[\left(\frac{\partial v}{\partial \mathbf{n}} \right)^2 - \left(\frac{\partial w}{\partial \mathbf{n}} \right)^2 \right] \\
& + r^2\, dr_1\, dr_2 \frac{\partial}{\partial \hat{\mathbf{x}}} \left\{ \|\nabla w\|^2 - \|\nabla v\|^2 \right\} \\
& + 2r^2\, dr_1 \left\{ \frac{\partial w}{\partial \mathbf{n}} \frac{\partial dw[dr_2]}{\partial \mathbf{n}} - \frac{\partial v}{\partial \mathbf{n}} \frac{\partial dv[dr_2]}{\partial \mathbf{n}} \right\} d\sigma,
\end{aligned} \tag{9}
$$

where all data have to be understood as traces on the boundary Γ*.*

Proof. The existence of a shape Hessian is provided by means of standard theory, cf. [9, 26]. To derive the explicit structure, we proceed similar to [10–11]by differentiating the shape gradient (8). The domain Ω respective boundary Γ can be identified with its parametrization, i.e., with the function $r : \mathbb{S} \to \Gamma$. Similarly, we can identify the perturbed domain Ω_ε respective boundary Γ_ε with the function $r_\varepsilon = r + \varepsilon dr_2$. Therefore, we find

$$
\begin{aligned}
& dJ(\Omega_\varepsilon)[dr_1] - dJ(\Omega_\varepsilon)[dr_1] \\
& \quad = \int_{\mathbb{S}} dr_1 \left\{ r_\varepsilon^2 \left[\left(\frac{\partial w_\varepsilon}{\partial \mathbf{n}_\varepsilon} \right)^2 - \left(\frac{\partial v_\varepsilon}{\partial \mathbf{n}_\varepsilon} \right)^2 \right] - r^2 \left[\left(\frac{\partial w}{\partial \mathbf{n}} \right)^2 - \left(\frac{\partial v}{\partial \mathbf{n}} \right)^2 \right] \right\} d\sigma,
\end{aligned}
$$

where v_ε and w_ε are the solutions of the state equation with respect to the perturbed domain Ω_ε and $\mathbf{n}_\varepsilon$ is the outer normal of Ω_ε at Γ_ε. Using Taylor's expansion

$$
r_\varepsilon^2 = r^2 + 2\varepsilon\, r\, dr_2 + \mathcal{O}(\varepsilon^2)
$$

yields

$$
\begin{aligned}
& dJ(\Omega_\varepsilon)[dr_1] - dJ(\Omega_\varepsilon)[dr_1] \\
& \quad = \int_{\mathbb{S}} dr_1 \left\{ 2r\varepsilon dr_2 \left[\left(\frac{\partial w_\varepsilon}{\partial \mathbf{n}_\varepsilon} \right)^2 - \left(\frac{\partial v_\varepsilon}{\partial \mathbf{n}_\varepsilon} \right)^2 \right] + \mathcal{O}(\varepsilon^2) \right\} d\sigma \\
& \quad + \int_{\mathbb{S}} dr_1 r^2 \left\{ \left[\left(\frac{\partial w_\varepsilon}{\partial \mathbf{n}_\varepsilon} \right)^2 - \left(\frac{\partial v_\varepsilon}{\partial \mathbf{n}_\varepsilon} \right)^2 \right] - r^2 \left[\left(\frac{\partial w}{\partial \mathbf{n}} \right)^2 - \left(\frac{\partial v}{\partial \mathbf{n}} \right)^2 \right] \right\} d\sigma.
\end{aligned}
$$

The first term in this expression will give the first term in (9). Hence, it remains to consider the difference

$$
\left(\frac{\partial v_\varepsilon}{\partial \mathbf{n}_\varepsilon} \right)^2 - \left(\frac{\partial v}{\partial \mathbf{n}} \right)^2 = \langle \nabla v_\varepsilon \big|_{\Gamma_\varepsilon}, \nabla v_\varepsilon \big|_{\Gamma_\varepsilon} \rangle - \langle \nabla v \big|_{\Gamma}, \nabla v \big|_{\Gamma} \rangle,
$$

since the corresponding term for w is treated in complete analogy. Observing $r_\varepsilon = r + \varepsilon dr_2$, we conclude by Taylor's expansion

$$\langle \nabla v_\varepsilon\big|_{\Gamma_\varepsilon}, \nabla v_\varepsilon\big|_{\Gamma_\varepsilon}\rangle = \langle \nabla v_\varepsilon\big|_{\Gamma}, \nabla v_\varepsilon\big|_{\Gamma}\rangle + 2\varepsilon dr_2 \frac{\partial}{\partial \widehat{\mathbf{x}}} \langle \nabla v_\varepsilon\big|_{\Gamma_\xi}, \nabla v_\varepsilon\big|_{\Gamma_\xi}\rangle,$$

where Γ_ξ is defined via the radial function $r_\xi = r + \xi dr_2$, $0 < \xi < \varepsilon$. Inserting now the local shape derivative (4)

$$\nabla v_\varepsilon\big|_{\Gamma} = \nabla v\big|_{\Gamma} + \varepsilon dr_2 \nabla dv[dr_2]\big|_{\Gamma} + \mathcal{O}(\varepsilon^2),$$

we arrive at

$$\begin{aligned}\left(\frac{\partial v_\varepsilon}{\partial \mathbf{n}}\right)^2 - \left(\frac{\partial v}{\partial \mathbf{n}}\right)^2 &= 2\varepsilon dr_2 \frac{\partial}{\partial \widehat{\mathbf{x}}} \langle \nabla v_\varepsilon\big|_{\Gamma_\xi}, \nabla v_\varepsilon\big|_{\Gamma_\xi}\rangle \\ &\quad + 2\varepsilon dr_2 \langle \nabla dv[dr_2]\big|_{\Gamma}, \nabla v\big|_{\Gamma}\rangle + \mathcal{O}(\varepsilon^2).\end{aligned}$$

Computing now $\lim_{\varepsilon\to 0}\{dJ(\Omega_\varepsilon)[dr_1] - dJ(\Omega_\varepsilon)[dr_1]\}/\varepsilon$ proves the assertion due to

$$\langle \nabla dv[dr_2]\big|_{\Gamma}, \nabla v\big|_{\Gamma}\rangle = \frac{\partial v}{\partial \mathbf{n}} \langle \nabla dv[dr_2]\big|_{\Gamma}, \mathbf{n}\rangle = \frac{\partial v}{\partial \mathbf{n}} \frac{\partial dv[dr_2]}{\partial \mathbf{n}}.$$

□

We like to stress that we have proven in [14]that the shape Hessian at the optimal domain $\Omega^\star$ is a compact mapping $H^{1/2}(\Gamma^\star) \to H^{-1/2}(\Gamma^\star)$, i.e., in its natural energy space. This issues from the fact that it holds $\partial v/\partial \mathbf{n} = \partial w/\partial \mathbf{n}$ on $\Gamma^\star$ due to the necessary condition (6). Hence, the first two terms in (9) cancel out and only the third term remains containing the difference $\partial dv[dr]/\partial \mathbf{n} - \partial dw[dr]/\partial \mathbf{n}$. This difference yields the compactness since the local shape derivatives differ only from the boundary conditions on Σ, cf. (4). As a main consequence, the known illposedness of the identification problem in EIT is strongly related to the illposedness of the optimization problem (1), (2). We refer the reader to [14]for the details.

1.3 Reformulating the shape Hessian

This subsection is intended to transform the second term of the shape Hessian (9) such that it is computable. For sake of brevity, we formulate the next results only with respect to v. But, of course, the equivalent results are valid also with respect to w.

LEMMA 2 *Let the normalized tangent* $\mathbf{t}$ *in the point* $\mathbf{x} = r(\widehat{\mathbf{x}}) \cdot \widehat{\mathbf{x}} \in \Gamma$ *be defined by*

$$\mathbf{t} = \frac{\mathbf{n} \times (\widehat{\mathbf{x}} \times \mathbf{n})}{\|\mathbf{n} \times (\widehat{\mathbf{x}} \times \mathbf{n})\|} = \frac{\|\nabla_{\mathbb{S}} r(\widehat{\mathbf{x}})\|^2 \widehat{\mathbf{x}} + r \nabla_{\mathbb{S}} r(\widehat{\mathbf{x}})}{\|\nabla_{\mathbb{S}} r(\widehat{\mathbf{x}})\| \sqrt{r^2(\widehat{\mathbf{x}}) + \|\nabla_{\mathbb{S}} r(\widehat{\mathbf{x}})\|^2}}.$$

Then, on Γ *there holds the identity*

$$\frac{\partial}{\partial\widehat{\mathbf{x}}}\|\nabla v\|^2 = 2\frac{\partial v}{\partial\mathbf{n}}\left\{\frac{\|\nabla_{\mathbb{S}} r(\widehat{\mathbf{x}})\|}{\sqrt{r^2(\widehat{\mathbf{x}})+\|\nabla_{\mathbb{S}} r(\widehat{\mathbf{x}})\|^2}}\frac{\partial^2 v}{\partial\mathbf{n}\partial\mathbf{t}} - \frac{r(\widehat{\mathbf{x}})}{\sqrt{r^2(\widehat{\mathbf{x}})+\|\nabla_{\mathbb{S}} r(\widehat{\mathbf{x}})\|^2}}\frac{\partial^2 v}{\partial\mathbf{n}^2}\right\},$$

where $\partial^2 v/\partial\mathbf{n}^2 := \langle\nabla^2 v\cdot\mathbf{n},\mathbf{n}\rangle$ *and* $\partial^2 v/(\partial\mathbf{n}\partial\mathbf{t}) := \langle\nabla^2 v\cdot\mathbf{n},\mathbf{t}\rangle$.

Proof. We decompose the spatial directions into the normal $\mathbf{n}$ in the point $\mathbf{x}\in\Gamma$ and two orthonormal tangential directions

$$\mathbf{s} = \frac{\widehat{\mathbf{x}}\times\mathbf{n}}{\|\widehat{\mathbf{x}}\times\mathbf{n}\|}, \qquad \mathbf{t} = \frac{\mathbf{n}\times(\widehat{\mathbf{x}}\times\mathbf{n})}{\|\mathbf{n}\times(\widehat{\mathbf{x}}\times\mathbf{n})\|}.$$

Note that

$$\mathbf{n}\times(\widehat{\mathbf{x}}\times\mathbf{n}) = \widehat{\mathbf{x}} - \langle\widehat{\mathbf{x}},\mathbf{n}\rangle\cdot\mathbf{n} = \frac{\|\nabla_{\mathbb{S}} r(\widehat{\mathbf{x}})\|^2\widehat{\mathbf{x}} + r\nabla_{\mathbb{S}} r(\widehat{\mathbf{x}})}{r^2(\widehat{\mathbf{x}})+\|\nabla_{\mathbb{S}} r(\widehat{\mathbf{x}})\|^2},$$
$$\|\mathbf{n}\times(\widehat{\mathbf{x}}\times\mathbf{n})\| = \frac{\|\nabla_{\mathbb{S}} r(\widehat{\mathbf{x}})\|}{\sqrt{r^2(\widehat{\mathbf{x}})+\|\nabla_{\mathbb{S}} r(\widehat{\mathbf{x}})\|^2}},$$

and hence

$$\mathbf{t} = \frac{\|\nabla_{\mathbb{S}} r(\widehat{\mathbf{x}})\|^2\widehat{\mathbf{x}} + r\nabla_{\mathbb{S}} r(\widehat{\mathbf{x}})}{\|\nabla_{\mathbb{S}} r(\widehat{\mathbf{x}})\|\sqrt{r^2(\widehat{\mathbf{x}})+\|\nabla_{\mathbb{S}} r(\widehat{\mathbf{x}})\|^2}}.$$

The ansatz

$$\widehat{\mathbf{x}} = \alpha\mathbf{n} + \beta\mathbf{s} + \gamma\mathbf{t}$$

leads to

$$\alpha = -\frac{r(\widehat{\mathbf{x}})}{\sqrt{r^2(\widehat{\mathbf{x}})+\|\nabla_{\mathbb{S}} r(\widehat{\mathbf{x}})\|^2}}, \qquad \gamma = \frac{\|\nabla_{\mathbb{S}} r(\widehat{\mathbf{x}})\|}{\sqrt{r^2(\widehat{\mathbf{x}})+\|\nabla_{\mathbb{S}} r(\widehat{\mathbf{x}})\|^2}},$$

and $\beta = 0$ since $\widehat{\mathbf{x}}\perp\widehat{\mathbf{x}}\times\mathbf{n}$. Consequently, we find

$$\begin{aligned}\frac{\partial}{\partial\widehat{\mathbf{x}}}\|\nabla v\|^2 &= \langle\nabla\|\nabla v\|^2,\widehat{\mathbf{x}}\rangle = 2\langle\nabla^2 v\cdot\widehat{\mathbf{x}},\nabla v\rangle = 2\frac{\partial v}{\partial\mathbf{n}}\langle\nabla^2 v\cdot\mathbf{n},\widehat{\mathbf{x}}\rangle\\ &= 2\frac{\partial v}{\partial\mathbf{n}}\left\{\frac{\|\nabla_{\mathbb{S}} r(\widehat{\mathbf{x}})\|}{\sqrt{r^2(\widehat{\mathbf{x}})+\|\nabla_{\mathbb{S}} r(\widehat{\mathbf{x}})\|^2}}\frac{\partial^2 v}{\partial\mathbf{n}\partial\mathbf{t}} - \frac{r(\widehat{\mathbf{x}})}{\sqrt{r^2(\widehat{\mathbf{x}})+\|\nabla_{\mathbb{S}} r(\widehat{\mathbf{x}})\|^2}}\frac{\partial^2 v}{\partial\mathbf{n}^2}\right\}.\end{aligned}$$

□

Hence, we have reduced the second term of the shape Hessian (9) to second order derivatives of the states. The next lemma shows how to compute the second order normal derivative.

LEMMA 3 *We denote by $\mathcal{H}$ the mean curvature. Then, on Γ there holds the identity*

$$\frac{\partial^2 v}{\partial \mathbf{n}^2} = 2\mathcal{H}\frac{\partial v}{\partial \mathbf{n}} \tag{10}$$

provided that $v \in C^2(\overline{\Omega})$.

Proof. Since $v \in C^2(\overline{\Omega})$, the Laplace equation holds up to the boundary Γ. It might be written as (see [26], for example)

$$\Delta v = \frac{\partial^2 v}{\partial \mathbf{n}^2} - 2\mathcal{H}\frac{\partial v}{\partial \mathbf{n}} + \Delta_\Gamma v = 0,$$

where Δ_Γ denotes the Laplace-Beltrami operator with respect to Γ. The homogenous Dirichlet condition on Γ implies $\Delta_\Gamma v = 0$ which yields immediately the assertion. □

Throughout the remainder of this paper we shall assume that the boundary manifold $\partial\Omega$ is given as a parametric surface consisting of smooth patches. More precisely, let $\square := [0,1]^2$ denote the unit square. The manifold $\partial\Omega = \Sigma \cup \Gamma \in \mathbb{R}^3$ is partitioned into a finite number of *patches*

$$\partial\Omega = \bigcup_{i=1}^{M} \Gamma_i, \qquad \Gamma_i = \gamma_i(\square), \qquad i = 1, 2, \dots, M, \tag{11}$$

where each $\gamma_i : \square \to \Gamma_i$ defines a diffeomorphism of $\square$ onto Γ_i. The intersection $\Gamma_i \cap \Gamma_{i'}$, $i \neq i'$, of the patches Γ_i and $\Gamma_{i'}$ is supposed to be either $\emptyset$ or a common edge or vertex.

Abbreviating for $\mathbf{s} = [s_1, s_2]^T \in \square$

$$\gamma_{i,j}(\mathbf{s}) := \frac{\partial \gamma_i(\mathbf{s})}{\partial s_j}, \qquad \gamma_{i,j,k}(\mathbf{s}) := \frac{\partial^2 \gamma_i(\mathbf{s})}{\partial s_j \partial s_k}, \qquad j,k = 1,2,$$

the first and second fundamental tensors of differential geometry are given by

$$\mathbf{K}_i(\mathbf{s}) = \left[\langle \gamma_{i,j}(\mathbf{s}), \gamma_{i,k}(\mathbf{s})\rangle\right]_{j,k=1,2}, \qquad \mathbf{L}_i(\mathbf{s}) = \left[\langle \mathbf{n}, \gamma_{i,j,k}(\mathbf{s})\rangle\right]_{j,k=1,2}.$$

Using these definitions, the mean curvature involved in (10) reads as (cf. [5])

$$\mathcal{H}\big(\gamma_i(\mathbf{s})\big) = \frac{1}{2}\,\mathrm{trace}\,\big(\mathbf{K}_i^{-1}(\mathbf{s})\mathbf{L}_i(\mathbf{s})\big).$$

Moreover, consider a function $u \in H^1(\partial\Omega)$ which is defined via parametrization, i.e., we have functions $\phi_i : \square \to \mathbb{R}$ satisfying $u \circ \gamma_i = \phi_i$, $i = 1, 2, \dots, M$. Then, according to [5], the surface gradient $\nabla_{\partial\Omega} u$ is defined as follows

$$\nabla_{\partial\Omega} u\big(\gamma_i(\mathbf{s})\big) = \big[\gamma_{i,1}(\mathbf{s}), \gamma_{i,2}(\mathbf{s})\big]\mathbf{K}_i^{-1}(\mathbf{s}) \begin{bmatrix} \frac{\partial \phi_i(\mathbf{s})}{\partial s_1} \\ \frac{\partial \phi_i(\mathbf{s})}{\partial s_2} \end{bmatrix}. \tag{12}$$

With these preperations at hand, we are able to prove the next lemma. We mention that it makes essentially use of the homogenous Dirichlet boundary conditions of v on Γ.

LEMMA 4 *On Γ there holds the identity*

$$\frac{\partial^2 v}{\partial \mathbf{n} \partial \mathbf{t}} = \Big\langle \nabla_\Gamma \frac{\partial v}{\partial \mathbf{n}}, \mathbf{t} \Big\rangle.$$

Proof. Invoking the parametrization, we find

$$\frac{\partial}{\partial s_1}\frac{\partial v}{\partial \mathbf{n}} = \frac{\partial}{\partial s_1}\langle \nabla v, \mathbf{n}\rangle = \langle \nabla^2 v \cdot \mathbf{n}, \gamma_{i,1}\rangle + \Big\langle \nabla v, \frac{\partial}{\partial s_1}\mathbf{n} \Big\rangle.$$

From

$$\begin{aligned} \frac{\partial}{\partial s_1}\mathbf{n} &= \frac{\partial}{\partial s_1}\frac{\gamma_{i,1} \times \gamma_{i,2}}{\|\gamma_{i,1} \times \gamma_{i,2}\|} \\ &= \frac{1}{\|\gamma_{i,1} \times \gamma_{i,2}\|}\left\{ \frac{\partial}{\partial s_1}(\gamma_{i,1} \times \gamma_{i,2}) - \Big\langle \mathbf{n}, \frac{\partial}{\partial s_1}(\gamma_{i,1} \times \gamma_{i,2}) \Big\rangle \cdot \mathbf{n} \right\} \end{aligned}$$

and

$$\Big\langle \nabla v, \frac{\partial}{\partial s_1}(\gamma_{i,1} \times \gamma_{i,2}) \Big\rangle = \frac{\partial v}{\partial \mathbf{n}} \Big\langle \mathbf{n}, \frac{\partial}{\partial s_1}(\gamma_{i,1} \times \gamma_{i,2}) \Big\rangle$$

we conclude

$$\Big\langle \nabla v, \frac{\partial}{\partial s_1}\mathbf{n} \Big\rangle = 0.$$

In complete analogy one infers the analogous result with respect to the derivative $\partial/\partial s_2$ such that we arrive at

$$\frac{\partial}{\partial s_1}\frac{\partial v}{\partial \mathbf{n}} = \langle \nabla^2 v \cdot \mathbf{n}, \gamma_{i,1}\rangle, \qquad \frac{\partial}{\partial s_2}\frac{\partial v}{\partial \mathbf{n}} = \langle \nabla^2 v \cdot \mathbf{n}, \gamma_{i,2}\rangle.$$

Next, defining the two tangential vectors $\widetilde{\gamma}_{i,1}$ and $\widetilde{\gamma}_{i,2}$ via

$$\left[\widetilde{\gamma}_{i,1}, \widetilde{\gamma}_{i,2}\right] := \left[\gamma_{i,1}, \gamma_{i,2}\right]\mathbf{K}_i^{-1}$$

one readily verifies

$$\langle \gamma_{i,k}, \widetilde{\gamma}_{i,l}\rangle = \delta_{j,k}, \qquad k,l = 1,2.$$

Hence, we can rewrite the tangent $\mathbf{t}$ by

$$\mathbf{t} = \langle \mathbf{t}, \widetilde{\gamma}_{i,1}\rangle\gamma_{i,1} + \langle \mathbf{t}, \widetilde{\gamma}_{i,2}\rangle\gamma_{i,2},$$

which implies

$$\begin{aligned}\frac{\partial^2 v}{\partial \mathbf{n}\partial \mathbf{t}} &= \langle \nabla^2 v\cdot\mathbf{n}, \mathbf{t}\rangle = \langle \nabla^2 v\cdot\mathbf{n}, \gamma_{i,1}\rangle\langle \mathbf{t}, \widetilde{\gamma}_{i,1}\rangle + \langle \nabla^2 v\cdot\mathbf{n}, \gamma_{i,2}\rangle\langle \mathbf{t}, \widetilde{\gamma}_{i,2}\rangle \\ &= \left\langle \left[\gamma_{i,1}, \gamma_{i,2}\right]\mathbf{K}_i^{-1}\begin{bmatrix}\langle \nabla^2 v\cdot\mathbf{n}, \gamma_{i,1}\rangle \\ \langle \nabla^2 v\cdot\mathbf{n}, \gamma_{i,2}\rangle\end{bmatrix}, \mathbf{t}\right\rangle = \left\langle \nabla_\Gamma \frac{\partial v}{\partial \mathbf{n}}, \mathbf{t}\right\rangle.\end{aligned}$$

□

We now combine the Lemmata 2, 3 and 4 and derive the final result.

COROLLARY 5 *The shape Hessian* (9) *is equivalent to*

$$\begin{aligned} d^2J(\Omega)[dr_1, dr_2] = \int_{\mathbb{S}} & 2r\, dr_1\, dr_2 \left[1 - \frac{2\mathcal{H}r^2}{\sqrt{r^2 + \|\nabla_{\mathbb{S}} r\|^2}}\right] \\ & \cdot \left[\left(\frac{\partial v}{\partial \mathbf{n}}\right)^2 - \left(\frac{\partial w}{\partial \mathbf{n}}\right)^2\right] \\ & + 2r^2\, dr_1\, dr_2 \left[\frac{\partial v}{\partial \mathbf{n}}\left\langle \nabla_\Gamma \frac{\partial v}{\partial \mathbf{n}}, \mathbf{n}\times(\widehat{\mathbf{x}}\times\mathbf{n})\right\rangle - \frac{\partial w}{\partial \mathbf{n}}\left\langle \nabla_\Gamma \frac{\partial w}{\partial \mathbf{n}}, \mathbf{n}\times(\widehat{\mathbf{x}}\times\mathbf{n})\right\rangle\right] \\ & + 2r^2\, dr_1 \left[\frac{\partial w}{\partial \mathbf{n}}\frac{\partial dw[dr_2]}{\partial \mathbf{n}} - \frac{\partial v}{\partial \mathbf{n}}\frac{\partial dv[dr_2]}{\partial \mathbf{n}}\right] d\sigma. \end{aligned} \tag{13}$$

1.4 Boundary integral equations

In this subsection we compute the unknown boundary data of the state functions v and w by boundary integral equations. We introduce the single layer and the double layer operator with respect the boundaries $\Phi, \Psi \in \{\Gamma, \Sigma\}$ by

$$\begin{aligned}(V_{\Phi\Psi}u)(\mathbf{x}) &:= -\frac{1}{4\pi}\int_\Phi \frac{1}{\|\mathbf{x}-\mathbf{y}\|}u(\mathbf{y})d\sigma_{\mathbf{y}}, \qquad \mathbf{x}\in\Psi, \\ (K_{\Phi\Psi}u)(\mathbf{x}) &:= \frac{1}{4\pi}\int_\Phi \frac{\langle \mathbf{x}-\mathbf{y}, \mathbf{n}_{\mathbf{y}}\rangle}{\|\mathbf{x}-\mathbf{y}\|^3}u(\mathbf{y})d\sigma_{\mathbf{y}}, \qquad \mathbf{x}\in\Psi.\end{aligned}$$

Note that $V_{\Phi\Psi}$ denotes an operator of order -1 if $\Phi = \Psi$, i.e. $V_{\Phi\Phi} : H^{-1/2}(\Phi) \to H^{1/2}(\Phi)$, while it is an arbitrarily smoothing compact operator if $\Phi \neq \Psi$ since $\operatorname{dist}(\Gamma, \Sigma) > 0$. Likewise, if $\Sigma, \Gamma \in C^2$, the double layer operator $K_{\Phi\Phi} : H^{1/2}(\Phi) \to H^{1/2}(\Phi)$ is compact while it smoothes arbitrarily if $\Phi \neq \Psi$. We refer the reader to [5, 18, 23]for a detailed description of boundary integral equations.

The normal derivative of w is given by the Dirichlet-to-Neumann map

$$\begin{bmatrix} V_{\Gamma\Gamma} & V_{\Sigma\Gamma} \\ V_{\Gamma\Sigma} & V_{\Sigma\Sigma} \end{bmatrix} \begin{bmatrix} \frac{\partial w}{\partial \mathbf{n}}\big|_\Gamma \\ \frac{\partial w}{\partial \mathbf{n}}\big|_\Sigma \end{bmatrix} = \begin{bmatrix} 1/2 + K_{\Gamma\Gamma} & K_{\Sigma\Gamma} \\ K_{\Gamma\Sigma} & 1/2 + K_{\Sigma\Sigma} \end{bmatrix} \begin{bmatrix} 0 \\ f \end{bmatrix}, \tag{14}$$

cf. (1). Likewise, the unknown boundary data of v are determined by

$$\begin{bmatrix} V_{\Gamma\Gamma} & -K_{\Sigma\Gamma} \\ -V_{\Gamma\Sigma} & 1/2 + K_{\Sigma\Sigma} \end{bmatrix} \begin{bmatrix} \frac{\partial v}{\partial \mathbf{n}}\big|_\Gamma \\ v|_\Sigma \end{bmatrix} = \begin{bmatrix} 1/2 + K_{\Gamma\Gamma} & -V_{\Sigma\Gamma} \\ -K_{\Gamma\Sigma} & V_{\Sigma\Sigma} \end{bmatrix} \begin{bmatrix} 0 \\ g \end{bmatrix}. \tag{15}$$

The unknown boundary data of the local shape derivatives $dv = dv[dr]$ and $dw = dw[dr]$ are derived by the boundary integral equations

$$\begin{aligned} &\begin{bmatrix} V_{\Gamma\Gamma} & V_{\Sigma\Gamma} \\ V_{\Gamma\Sigma} & V_{\Sigma\Sigma} \end{bmatrix} \begin{bmatrix} \frac{\partial dw}{\partial \mathbf{n}}\big|_\Gamma \\ \frac{\partial dw}{\partial \mathbf{n}}\big|_\Sigma \end{bmatrix} \\ &\qquad = \begin{bmatrix} 1/2 + K_{\Gamma\Gamma} & K_{\Sigma\Gamma} \\ K_{\Gamma\Sigma} & 1/2 + K_{\Sigma\Sigma} \end{bmatrix} \begin{bmatrix} -\langle \mathbf{V}, \mathbf{n} \rangle \frac{\partial w}{\partial \mathbf{n}}\big|_\Gamma \\ 0 \end{bmatrix} \end{aligned} \tag{16}$$

and

$$\begin{aligned} &\begin{bmatrix} V_{\Gamma\Gamma} & -K_{\Sigma\Gamma} \\ -V_{\Gamma\Sigma} & 1/2 + K_{\Sigma\Sigma} \end{bmatrix} \begin{bmatrix} \frac{\partial dv}{\partial \mathbf{n}}\big|_\Gamma \\ dv|_\Sigma \end{bmatrix} \\ &\qquad = \begin{bmatrix} 1/2 + K_{\Gamma\Gamma} & -V_{\Sigma\Gamma} \\ -K_{\Gamma\Sigma} & V_{\Sigma\Sigma} \end{bmatrix} \begin{bmatrix} -\langle \mathbf{V}, \mathbf{n} \rangle \frac{\partial v}{\partial \mathbf{n}}\big|_\Gamma \\ 0 \end{bmatrix}. \end{aligned} \tag{17}$$

2. Discretization

2.1 Finite dimensional approximation of boundaries

Since the infinite dimensional optimization problem cannot be solved directly, we replace it by a finite dimensional problem. Recall that the boundary Γ admits a unique representation

$$\Gamma = \left\{ r(\widehat{\mathbf{x}}) \cdot \widehat{\mathbf{x}} \in \mathbb{R}^3 \, : \, \widehat{\mathbf{x}} \in \mathbb{S} \right\}, \tag{18}$$

and the regularity $\Gamma \in C^{2,\alpha}$ is directly associated to $r \in C^{2,\alpha}(\mathbb{S})$. We now introduce the spherical harmonics.

For $n \in \mathbb{N}_0$ and $|m| \leq n$ consider the Legendre polynomials

$$P_n(t) := \frac{1}{2^n n!}\Big(\frac{d}{dt}\Big)^n (t^2-1)^n, \quad t \in \mathbb{R},$$

and the associated Legendre functions

$$P_n^{|m|}(t) := (1-t^2)^{|m|/2}\Big(\frac{d}{dt}\Big)^{|m|} P_n(t), \quad t \in \mathbb{R}.$$

Then, the spherical harmonics $Y_n^m : \mathbb{S} \to \mathbb{R}$ are given by

$$Y_n^m(\widehat{\mathbf{x}}) := \sqrt{\frac{2n+1}{4\pi}\frac{(n-|m|)!}{(n+|m|)!}} P_n^{|m|}(\widehat{x}_3) \begin{cases} \mathrm{Re}\,\big((\widehat{x}_1+i\widehat{x}_2)^m\big), & m \geq 0, \\ \mathrm{Im}\,\big((\widehat{x}_1+i\widehat{x}_2)^m\big), & m < 0. \end{cases}$$

Since the spherical harmonics are the restriction of homogeneous harmonical polynomials to the unit sphere, the radial function r in (18) admits a unique representation

$$r(\widehat{\mathbf{x}}) = \sum_{n=0}^{\infty} \sum_{m=-n}^{n} \alpha_{m,n} Y_n^m(\widehat{\mathbf{x}}), \quad \widehat{\mathbf{x}} \in \mathbb{S},$$

with certain numbers $\alpha_{m,n} \in \mathbb{R}$. Hence, it is reasonable to take a truncated series

$$r_N(\widehat{\mathbf{x}}) = \sum_{n=0}^{N} \sum_{m=-n}^{n} \alpha_{m,n} Y_n^m(\widehat{\mathbf{x}}), \quad \widehat{\mathbf{x}} \in \mathbb{S}, \tag{19}$$

as approximation of r. We mention that also other boundary representations like B-splines can be considered as well. The advantages of our approach is an exponential convergence $r_N \to r$ if the shape is analytical.

Since r_N has the $(N+1)^2$ degrees of freedom $a_{0,0}, a_{-1,1}, \ldots, a_{N,N}$, we arrive at a finite dimensional optimization problem in the open set

$$\Upsilon_N := \{(a_{0,0}, a_{-1,1}, \ldots, a_{N,N}) : r_N > 0 \text{ on } \mathbb{S} \text{ and } \operatorname{dist}(\Sigma, \Gamma) > 0\},$$

which is a subset of $\mathbb{R}^{(N+1)^2}$. Then, via the identification $r_N \Leftrightarrow \Omega_N$, the finite dimensional approximation of problem (2) reads as

$$J(\Omega_N) \to \min \tag{20}$$

The associated gradient $dJ(\Omega_N)[dr]$ and Hessian $d^2J(\Omega_N)[dr_1, dr_2]$ have to be computed with respect to all directions $dr, dr_1, dr_2 = Y_n^m(\mathbf{x})\mathbf{x}$, $m = -n, \ldots, n$, and $n = 0, \ldots, N$.

At the end of this subsection, we like to point out that a parametric representation in accordance with Subsection 1.1.3 can be constructed

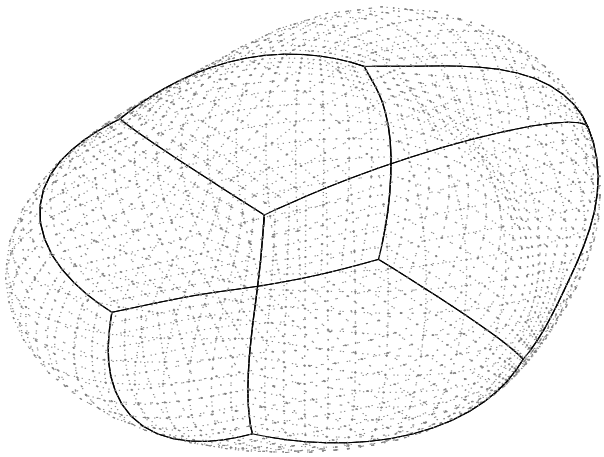

Figure 2. Parametric representation of Ω.

as follows. The cube $[-0.5, 0.5]^3$ consists of six patches. Each point $\mathbf{x} \in [-0.5, 0.5]^3$ can be lifted onto the boundary Γ via the operation

$$\mathbf{y}(\mathbf{x}) = r_N\Big(\frac{\mathbf{x}}{\|\mathbf{x}\|}\Big) \cdot \frac{\mathbf{x}}{\|\mathbf{x}\|} \in \Gamma. \tag{21}$$

That way, the surface is subdivided into six patches. The parametric representations $\gamma_i : \Gamma_i \to \Gamma$ can be easily derived from (21). In Figure 2 one finds an illustration of the proposed parametric representation.

2.2 Treating the optimization problem

The minimization problem defined by (20) implies to find its stationary points $\Omega^\star_{N_r}$

$$dJ(\Omega^\star_{N_r})[dr] = 0 \tag{22}$$

for all directions $dr = Y_n^m(\mathbf{x})\mathbf{x}$, $m = -n, \dots, n$, and $n = 0, \dots, N$. To solve (22), we consider on the one hand a method which is based only on first order information, namely a quasi Newton method updated by the inverse BFGS-rule without damping, see [16–17]for the details.

On the other hand, we perform a Newton method which we regularize since the shape Hessian is compact at the optimal domain $\Omega^\star$. Namely, abbreviating the discrete gradient by $\mathbf{G}_n$ and the associated Hessian by $\mathbf{H}_n$, we consider in the n-th iteration step the descent direction

$$\mathbf{h}_n := -(\mathbf{H}_n^2 + \alpha_n \mathbf{I})^{-1}\mathbf{H}_n\mathbf{G}_n,$$

where $\alpha_n > 0$ is an appropriately chosen regularization parameter. This descent direction $\mathbf{h}_n$ solves the minimization problem

$$\|\mathbf{H}_n\mathbf{h}_n - \mathbf{G}_n\|^2 + \alpha_n\|\mathbf{h}_n\|^2 \to \min$$

and corresponds to a Tikhinov regularization of equation (22). Moreover, note that we employ in both methods a quadratic line search with respect to the functional (2) based on the information of the actual value of the cost functional and its gradient, and on the value of the cost functional with respect to the new domain.

2.3 Numerical method to compute the state

We want to employ a boundary element method to compute the required boundary data of the state equations. Recall that we have introduced in Subsection 1.1.3 a parametric representation of boundary $\partial\Omega = \Gamma \cup \Sigma$ by quadriliteral patches. A mesh of level j on $\partial\Omega$ is then induced by dyadic subdivisions of depth j of the reference square $\square$ into 4^j squares. This generates $4^j M$ *elements* (or elementary domains). On the given mesh we consider on each boundary $\Phi \in \{\Gamma, \Sigma\}$ piecewise bilinear basis functions $\{\theta^\Phi_{j,k} : k \in \triangle^\Phi_j\}$, where $\triangle^\Phi_j$ denotes an appropriate index set.

For $\Phi, \Psi \in \{\Sigma, \Gamma\}$, we introduce the system matrices

$$\mathbf{V}_{\Phi\Psi} = \frac{1}{4\pi}\left[\int_\Psi\int_\Phi \frac{1}{\|\mathbf{x}-\mathbf{y}\|}\theta^\Phi_i(\mathbf{y})\theta^\Psi_j(\mathbf{x})d\sigma_\mathbf{y}d\sigma_\mathbf{x}\right]_{i\in\triangle^\Phi_j,\, j\in\triangle^\Psi_j},$$

$$\mathbf{K}_{\Phi\Psi} = \frac{1}{4\pi}\left[\int_\Psi\int_\Phi \frac{\langle \mathbf{x}-\mathbf{y}, \mathbf{n}_\mathbf{y}\rangle}{\|\mathbf{x}-\mathbf{y}\|^3}\theta^\Phi_i(\mathbf{y})\theta^\Psi_j(\mathbf{x})d\sigma_\mathbf{y}d\sigma_\mathbf{x}\right]_{i\in\triangle^\Phi_j,\, j\in\triangle^\Psi_j},$$

and the mass matrices

$$\mathbf{M}_\Phi = \left[\int_\Phi \theta^\Phi_i(\mathbf{x})\theta^\Phi_j(\mathbf{x})d\sigma_\mathbf{x}\right]_{i,j\in\triangle^\Phi_j},$$

and the load vectors of Dirichlet data f_Φ and Neumann data g_Φ

$$\mathbf{f}_\Phi = \left[\int_\Phi \theta^\Phi_i(\mathbf{x})f(\mathbf{x})d\sigma_\mathbf{x}\right]_{i\in\triangle^\Phi_j}, \qquad \mathbf{g}_\Phi = \left[\int_\Phi \theta^\Phi_i(\mathbf{x})g(\mathbf{x})d\sigma_\mathbf{x}\right]_{i\in\triangle^\Phi_j}.$$

Then, the linear system of equations

$$\begin{bmatrix}\mathbf{V}_{\Gamma\Gamma} & \mathbf{V}_{\Sigma\Gamma}\\ \mathbf{V}_{\Gamma\Sigma} & \mathbf{V}_{\Sigma\Sigma}\end{bmatrix}\begin{bmatrix}\mathbf{a}_\Gamma\\ \mathbf{a}_\Sigma\end{bmatrix} = \begin{bmatrix}1/2\mathbf{M}_\Gamma + \mathbf{K}_{\Gamma\Gamma} & \mathbf{K}_{\Sigma\Gamma}\\ \mathbf{K}_{\Gamma\Sigma} & 1/2\mathbf{M}_\Sigma + \mathbf{K}_{\Sigma\Sigma}\end{bmatrix}\begin{bmatrix}\mathbf{M}^{-1}_\Gamma\mathbf{f}_\Gamma\\ \mathbf{M}^{-1}_\Sigma\mathbf{f}_\Sigma\end{bmatrix}, \tag{23}$$

gives us the Neumann data $a_\Gamma = \sum_{i\in\triangle_j^\Gamma}[\mathbf{a}_\Gamma]_i\theta_i^\Gamma$ on Γ and $a_\Sigma = \sum_{i\in\triangle_j^\Sigma}[\mathbf{a}_\Sigma]_i\theta_i^\Sigma$ on Σ from the Dirichlet data on Γ and Σ. Likewise, the system

$$\begin{bmatrix} \mathbf{V}_{\Gamma\Gamma} & -\mathbf{K}_{\Sigma\Gamma} \\ -\mathbf{V}_{\Gamma\Sigma} & 1/2\mathbf{M}_\Sigma + \mathbf{K}_{\Sigma\Sigma} \end{bmatrix} \begin{bmatrix} \mathbf{b}_\Gamma \\ \mathbf{a}_\Gamma \end{bmatrix} = \begin{bmatrix} 1/2\mathbf{M}_\Gamma + \mathbf{K}_{\Gamma\Gamma} & -\mathbf{V}_{\Sigma\Gamma} \\ -\mathbf{K}_{\Gamma\Sigma} & \mathbf{V}_{\Sigma\Sigma} \end{bmatrix} \begin{bmatrix} \mathbf{M}_\Gamma^{-1}\mathbf{g}_\Gamma \\ \mathbf{M}_\Sigma^{-1}\mathbf{f}_\Sigma \end{bmatrix}, \tag{24}$$

yields the Dirichlet data $b_\Gamma = \sum_{i\in\triangle_j^\Gamma}[\mathbf{b}_\Gamma]_i\theta_i^\Gamma$ on Γ and the Neumann data $a_\Sigma = \sum_{i\in\triangle_j^\Sigma}[\mathbf{a}_\Sigma]_i\theta_i^\Sigma$ on Σ from the Neumann data $\mathbf{g}_\Gamma$ on Γ and the Dirichlet data $\mathbf{f}_\Sigma$ on Σ. Note that we plugged in the L^2-orthogonal projection involving $\mathbf{M}_\Phi^{-1}$ to decouple the data vectors from the boundary integral operators on the right hand side, see also [12–13].

Using the traditional piecewise bilinear nodal basis functions leads to the traditional boundary element method. Then, the system matrices are densely populated and we end up with an at least quadratic complexity for computing the approximate solution of (23) and (24), i.e., the computational work scales like $\mathcal{O}\big((|\triangle_j^\Gamma| + |\triangle_j^\Sigma|)^2\big) = \mathcal{O}(16^j)$.

We employ instead appropriate *biorthogonal spline wavelets* as constructed in several papers, see e.g. [8, 20, 21]. Then, we obtain quasi–sparse system matrices having only $\mathcal{O}(|\triangle_j^\Gamma| + |\triangle_j^\Sigma|) = \mathcal{O}(4^j)$ relevant matrix coefficients. Applying the matrix compression strategy developed in [6, 25]combined with an exponentially convergent *hp*–quadrature method [19], the wavelet Galerkin scheme produces the approximate solution of (23) and (24) within linear complexity. In particular, due to the norm equivalences of the wavelet bases, the diagonal of the system matrices define appropriate preconditioners [7, 25]

We mention that the appearing system matrices have to be computed only once for each domain while the systems (23) and (24) have to be solved $(N+1)^2$ times with different right hand sides to obtain the Neumann data of the local shape derivates. We emphazise that the iterative solution is much faster for the very sparsified system in wavelet coordinates compared to the dense system arising from the traditional boundary element method.

3. Numerical results

We choose D as the cube $[-1,1]^3$ and a inclusion S centered in $\mathbf{0}$ as shown in Figure 3. The Dirichlet data f are chosen as $(4x^2 - 3y^2 - z^2)|_\Sigma$ while the Neumann data g are computed numerically with appropriate accuracy. We use a sphere, also centered in $\mathbf{0}$, near the optimal domain as initial guess, cf. 3. The numerical setting is as follows. We

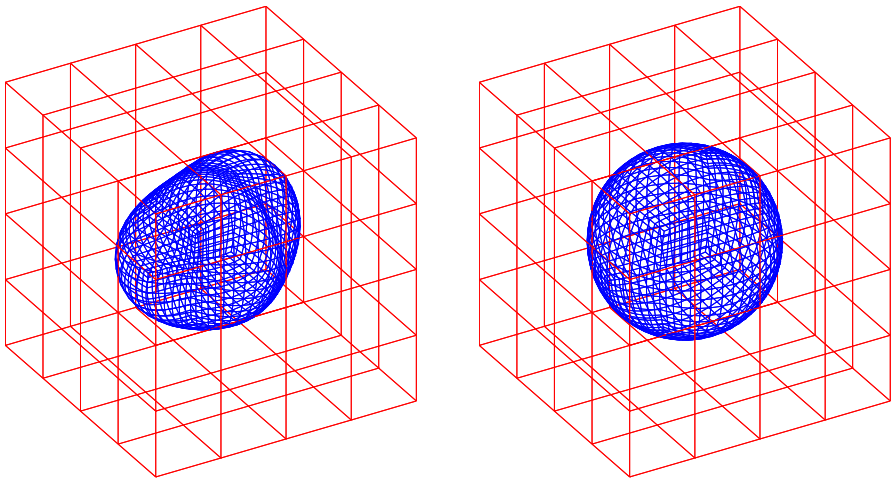

Figure 3. The exact inlcusion (left) and the initial guess (right).

choose $N = 5$, i.e. 36 spherical harmonics to represent the boundary Γ. The cube is represented by six patches, that are twelve patches in all to represent the boundary $\partial\Omega$. The Galerkin discretization is performed on the mesh of level 4 which yields 3468 piecewise bilinear boundary elements. We follow [14]and choose $\alpha_n = 2^{-n}$ in the n-th step of the regularized Newton method. Thus, in each step we reduce the regularization parameter by the factor 2. Again this choice turns out to be very efficient.

In the left picture of Figure 4 the history of the shape error is plotted, measured by the ℓ^2-norm of the coeffcients associated with the spherical harmonics. The dashed line corresponds to the quasi Newton method while the solid line belongs to the regularized Newton method. The regularized Newton method requires only 30 iteration steps to achieve the accuracy offered by the underlying discretization which is indicated by stagnation of convergence about the shape error $5 \cdot 10^{-5}$, cf. Figure 4. In contrast, the quasi Newton method does not compute the optimal shape so accurate even after 50 iterations. Its convergence is much slower compared to the regularized Newton method. It realizes within 50 iterations only an approximation error of about $5 \cdot 10^{-2}$. Nearly the same behaviour can be observed in the history of the cost functional, that is the left picture of Figure 4. We emphasize that the regularized Newton scheme realizes an value of $5 \cdot 10^{-11}$ in constrast to $3 \cdot 10^{-5}$ which is achieved by the quasi Newton method. The final approximations to the optimal domains can be found in Figure 5.

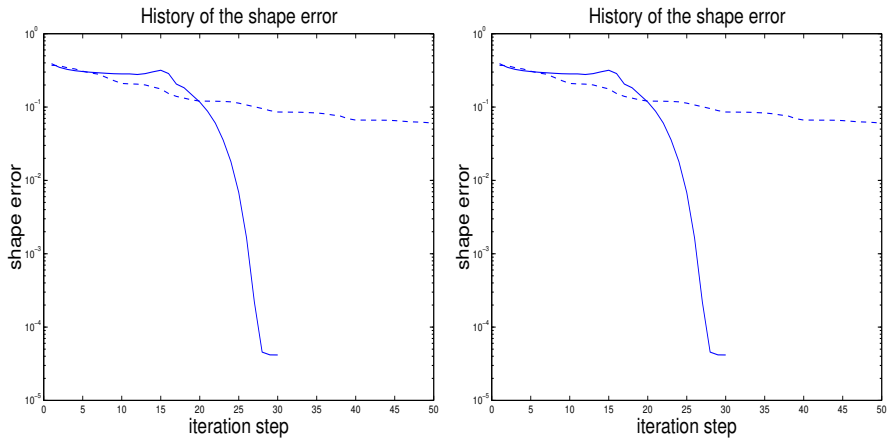

Figure 4. Shape error (left) and cost functional (right) versus iteration step.

The Newton method consumes about 1.5 hours computing time at a standard personal computer, the quasi Newton method requires even 10% more cpu-time. We mention that about 80 seconds are required to compute the system matrices and to solve them with one right hand side each. Therefore, one quasi-Newton step requires about 80 seconds if the line search becomes not active. Whereas a Newton step requires about twice that time which issues mainly from the multiple iterative solution of the linear equation systems to compute the local shape derivatives. But we emphasize that in the present example the regularized Newton scheme requires never the line search.

4. Conclusion

In the present paper we considered second order methods for the identification of voids or inclusions. The problem under consideration is well known to be severely ill-posed. Since the shape Hessian is compact at the optimal domain, we propose a regularized Newton method for the resolution of the inclusion. The numerical example shows that the proposed regularized Newton method converges faster and yields a more accurate solution compared to a quasi Newton scheme.

References

[1] G. Alessandrini, V. Isakov, and J. Powell. Local uniqueness in the inverse problem with one measurement. *Trans. Am. Math. Soc.*, 347:3031–3041, 1995.

[2] M. Brühl. Explicit characterization of inclusions in electrical impedance tomography. *SIAM J. Math. Anal.*, 32:1327–1341, 2001.

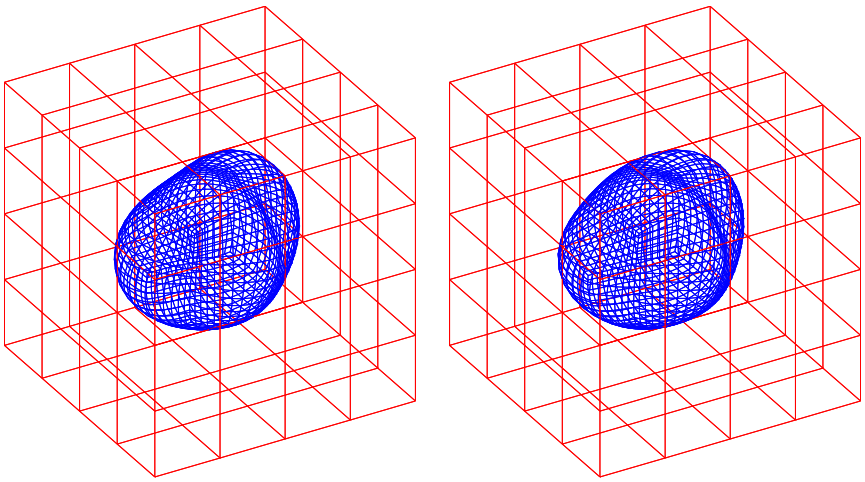

Figure 5. Approximate solutions produces by the regualrized Newton method (left) and the quasi Newton method (right).

[3] M. Brühl and M. Hanke. Numerical implementation of two noniterative methods for locating inclusions by impedance tomography. *Inverse Problems*, 16:1029–1042, 2000.

[4] R. Chapko and R. Kress. A hybrid method for inverse boundary value problems in potential theory, 2003. to appear.

[5] K. Colton and R. Kress. *Integral equation methods in scattering theory.* Pure and Applied Mathematics. Wiley, Chichester, 1983.

[6] W. Dahmen, H. Harbrecht, and R. Schneider. Compression techniques for boundary integral equations – optimal complexity estimates. Technical Report SFB 393/02-06, TU Chemnitz, Institute of Mathematics, D-09107 Chemnitz, 2002. submitted for publication.

[7] W. Dahmen and A. Kunoth. Multilevel preconditioning. *Numer. Math.*, 63:315–344, 1992.

[8] W. Dahmen, A. Kunoth, and K. Urban. Biorthogonal spline-wavelets on the interval – stability and moment conditions. *Appl. Comp. Harm. Anal.*, 6:259–302, 1999.

[9] M. Delfour and J.-P. Zolesio. *Shapes and Geometries.* SIAM, Philadelphia, 2001.

[10] K. Eppler. Boundary integral representations of second derivatives in shape optimization. *Discussiones Mathematicae (Differential Inclusion Control and Optimization)*, 20:63–78, 2000.

[11] K. Eppler. Optimal shape design for elliptic equations via BIE-methods. *J. of Applied Mathematics and Computer Science*, 10:487–516, 2000.

[12] K. Eppler and H. Harbrecht. 2nd order shape optimization using wavelet BEM. Technical Report 06-2003, TU Berlin, Institute of Mathematics, Str. d. 17. Juni, D-10623 Berlin, 2003. submitted for publication.

[13] K. Eppler and H. Harbrecht. Numerical solution of elliptic shape optimization problems using wavelet-based BEM. *Optim. Methods Softw.*, 18:105–123, 2003.

[14] K. Eppler and H. Harbrecht. A regularized Newton method in electrical impedance tomography using shape Hessian information. Technical Report 943, WIAS Berlin, Mohrenstr. 39, D-10117 Berlin, 2004. submitted for publication.

[15] A. Friedman and V. Isakov. On the uniqueness in the inverse conductivity problem with one measurement. *Indiana Univ. Math. J.*, 38:563–579, 1989.

[16] P.E. Gill, W. Murray, and M.H. Wright. *Practical Optimization*. Academic Press, New York, 1981.

[17] Ch. Grossmann and J. Terno. *Numerik der Optimierung*. B.G. Teubner, Stuttgart, 1993.

[18] W. Hackbusch. *Integralgleichungen*. B.G. Teubner, Stuttgart, 1989.

[19] H. Harbrecht and R. Schneider. Wavelet Galerkin schemes for boundary integral equations – Implementation and quadrature. Technical Report SFB 393/02-21, TU Chemnitz, Institute of Mathematics, D-09107 Chemnitz, 2002. submitted for publication.

[20] H. Harbrecht and R. Schneider. Biorthogonal wavelet bases for the boundary element method. *Math. Nachr.*, 269-270:167–188, 2004.

[21] Helmut Harbrecht. *Wavelet Galerkin schemes for the boundary element method in three dimensions*. PhD thesis, Technical University of Chemnitz, Str. d. Nationen 62, D-09111 Chemnitz, 2001.

[22] F. Hettlich and W. Rundell. The determination of a discontinuity in a conductivity from a single boundary measurement. *Inverse Problems*, 14:67–82, 1998.

[23] R. Kress. *Linear Integral Equations*. Springer, Berlin-Heidelberg, 1989.

[24] J.-R. Roche and J. Sokolowski. Numerical methods for shape identification problems. *Control Cybern.*, 25:867–894, 1996.

[25] R. Schneider. *Multiskalen- und Wavelet-Matrixkompression: Analysisbasierte Methoden zur Lösung großer vollbesetzter Gleichungssysteme*. B.G. Teubner, Stuttgart, 1998.

[26] J. Sokolowski and J.-P. Zolesio. *Introduction to shape optimization*. Springer, Berlin, 1992.